Influence of the sensitizer reduction potential on the sensitivity of photorefractive polymer composites

Koeber, Sebastian; Gallego-Gomez, Francisco; Salvador, Michael; Kooistra, Floris B.; Hummelen, Jan; Aleman, Karina; Mansurova, Svetlana; Meerholz, Klaus

Published in:
Journal of Materials Chemistry

DOI:
10.1039/c0jm01208d

Publication date:
2010

Influence of the sensitizer reduction potential on the sensitivity of photorefractive polymer composites†

Sebastian Köber,[a] Francisco Gallego-Gomez,‡[a] Michael Salvador,[a] Floris B. Kooistra,[b] Jan C. Hummelen,[b] Karina Aleman,[c] Svetlana Mansurova[c] and Klaus Meerholz*[c]

Received 26th April 2010, Accepted 28th May 2010
DOI: 10.1039/c0jm01208d

We report on a series of near infrared (NIR)-sensitive photorefractive polymer composites (PPCs) based on the hole-conducting polymer PF6-TPD, which are sensitized by soluble fullerene-derivatives as electron-accepting agents. We demonstrate a direct correlation between the electron accepting capability of the sensitizer and the holographic response time. The holographic recording speed is found to improve by one order of magnitude when lowering the reduction potential of the sensitizer by approx. 400 mV, while all other physical parameters of the materials remain essentially identical. Furthermore, the lifetime of the mobile charge carriers is found to correlate linearly with the reduction potential, thus indicating a decrease in recombination rates for stronger accepting capability of the sensitizer. Finally, we found that pre-illumination enhanced the holographic sensitivity. The effect is found to be most pronounced for the strongest acceptor due to reduced recombination of the preformed carriers. Overall, the PPCs reported here feature the currently highest sensitivity in the NIR spectral region.

Introduction

Photorefractive polymer composites (PPCs) are today among the most promising candidates for various holographic applications. Recent examples include a reconfigurable holographic display[1] and all-optical logic gates by photorefractive two-wave mixing.[2] Another exciting application is holographic optical coherence imaging (HOCI), which is capable of real-time imaging through turbid media by optical radiation.[3–5] For applications in medical diagnosis, the use of near infrared (NIR) light sources is required because of biological tissues' transparency window in the 700–900 nm range. Within this particular spectral range, PPCs generally lack sensitivity for fast holographic imaging purposes.

The photorefractive effect in organic materials biased by a dc-field involves charge-carrier photogeneration in the bright regions of an interference pattern and the subsequent displacement of the mobile charges (typically holes) due to field-induced drift. This charge separation leads to the formation of an internal space-charge field E_{SC}, which is phase-shifted relative to the interference pattern. In low-T_g materials, electro-optic chromophores are reoriented along the total field E_T, which is the vectorial sum of E_{SC} and the applied field E_{ext}. The change of refractive index Δn is then given through the quadratic electro-optic (Kerr-) effect and modulated birefringence.[6] The phase shift between the recorded refractive index modulation and the impinging interference pattern gives rise to asymmetric energy transfer from one write beam to the other, which is quantitatively accessible by the so-called two-beam coupling (2BC) gain coefficient Γ.

PPCs generally contain electrooptical chromophores in a photoconductive matrix (typically p-type hole conductors). Owing to the low intrinsic charge-generation efficiency of organic photoconductors in the visible and the NIR spectral range, sensitizers (typically n-type acceptors) are incorporated into the material. These components provide absorption at the desired wavelength and assist in photogeneration of charges. The interaction of the sensitizing agent with the charge transporting component is of paramount importance for the hologram-formation dynamics in the material, thus generally, the sensitizer must be selected for a specific photoconducting host and/or the wavelength of charge generation. Moreover, the sensitizer radical anion, formed upon illumination of the material and subsequent charge transfer to the transport matrix, has been identified as recombination trap for the mobile hole in the composite.[6]

Recent publications describing the influence of the sensitizing agent on the photorefractivity of carbazole-based polymeric composites can be found in ref. 7 and 8, respectively. For applications in the NIR (790–830 nm), the most common sensitizers are electron-accepting molecules like (2,4,7-trinitro-9-fluorenylidene)malononitrile (TNFM)[9–11] and C_{60}[6,12,13] or its soluble derivative [6,6]-phenyl-C_{61}-butyric acid methyl ester ([60]PCBM).[3,6,12,14,15] These are known to form charge-transfer (CT) complexes with certain donor-type molecules and polymers, which give rise to additional absorption at the desired wavelength. For example, in ref. 16 the CT complex of poly(*N*-vinylcarbazole) (PVK) with C_{60} and C_{70} was identified as the main precursor for charge generation.

Since the generation of charges depends on the donor capability of the hole-transporting matrix as well as the acceptor strength of

[a]*Chemistry Department, University of Cologne, Luxemburger Str. 116, 50939 Cologne, Germany. E-mail: klaus.meerholz@uni-koeln.de*
[b]*Molecular Electronics, Stratingh Institute for Chemistry & Zernike Institute for Advanced Materials, University of Groningen, Nijenborgh 4, 9747 AG Groningen, The Netherlands*
[c]*INAOE, Aparto Postal 51 y 216, Puebla, 72000, Mexico*

† Electronic supplementary information (ESI) available: Determination of τ_{50} and $E(\eta_{max})$ from measured data, comparison of pre-illuminated and non pre-illuminated data transients and the ratio of their respective sensitivities. See DOI: 10.1039/c0jm01208d

‡ Current adress: Instituto de Ciencia de Materiales de Madrid, Consejo Superior de Investigaciones Científicas, Campus de Cantoblanco, 28049 Madrid, Spain.

the sensitizer, both charge generation and recombination are affected by their relative ionization potentials. Hendrickx *et al.* demonstrated by photocurrent measurements[17] that lowering the ionization potential I_P of the hole-conducting matrix (a series of triarylamines) with respect to the sensitizers' (C_{60}) I_P enhances the photogeneration efficiency of the composite material under 633 nm illumination. Through chemical substitution with appropriate electron donating and withdrawing moieties, the ionization potential of the hole-conductor was varied by 0.25 eV, which was shown to enhance the photogeneration efficiency of the donor–acceptor complex from 6% (weakest donor) to 100% (best donor) with an applied field of 55 V μm^{-1}. The described experiments did, however, not involve any holographic measurements.

So far, no analogous examination on the influence of variations of the reduction potential on the photoelectric and holographic properties of the composites has been conducted.

We have recently introduced a novel hole-conducting matrix material, poly(*N*,*N*′-bis(4-hexylphenyl)-*N*′-(4-(9-phenyl-9*H*-fluoren-9-yl)phenyl)-4,4′-benzidine)[18] (PF6-TPD). In a previous study, we demonstrated efficient NIR holographic recording in the material by incorporating [60]PCBM as sensitizer,[4,5] an acceptor which is commonly used in organic bulk-heterojunction solar cells. In this work, we investigate a series of soluble fullerenes with higher as well as lower acceptor strength as alternative sensitizers. We demonstrate that variation of the sensitizers reduction potential by only *ca.* 400 mV yields one order of magnitude difference in the holographic response time. Also, the influence of the reduction potential on the impact of pre-illumination[3] on the sensitivity is discussed. Through supplementary photo-electromotive force (p-EMF) investigations, we further show that this improvement is closely related to an extended charge carrier (hole) lifetime due to reduced recombination rates.

Experimental

Material composition

The PPCs investigated in this work consisted of the hole-transporting polymer PF6-TPD as the matrix material (49 wt%).[18] Nonlinear optical response was achieved by including 25 wt% of each of the electro-optic chromophores 2,5-dimethyl-(4-*p*-nitrophenylazo)anisole (DMNPAA) and 3-methoxy-(4-*p*-nitrophenylazo)-anisole (MNPAA) into the polymer host. Since both chromophores feature oxidation potentials (1.21 V *vs.* Fc/Fc^+, ref. 6) higher than for PF6-TPD (0.25 V *vs.* Fc/Fc^+, ref. 24), they do not constitute hole traps within the charge-transporting manifold. If this was the case, deterioration of the materials' holographic response by accumulation of charges in combination with electron accepting molecules like C_{60}[13] or PCBM may occur. The composite was completed by 1 wt% of a fullerene as sensitizer. No plasticizer was added.

The reference composite was sensitized with [60]PCBM (**3** in Fig. 1). The other PPCs included derivatives of the [60]PCBM with a functionalized phenyl ring: 2,5-OMe-PCBM **1** and F5-PCBM **5**,[19] structures with modifications to the [60]fullerene core: azafulleroid **4** and a ketolactam quasifullerene **6**,[20] and, finally, higher fullerene derivatives: [70]PCBM **2** and [84]PCBM **7**.[21] This series of fullerenes varies by almost 400 mV in their first reduction potential from the worst (2,5-OMe-PCBM) to the best electron acceptor ([84]PCBM). All chemical structures are depicted in Fig. 1.

Sample preparation

All components were dissolved in spectroscopy-grade dichloromethane, the solvent was evaporated and the materials homogenized. The composite was sandwiched between two ITO-coated glass sheets, melted at 150 °C and pressed to an uniform thickness of $d = 106$ μm, ensured by glassy spacer beads. For p-EMF and absorption measurements, 37 μm thick samples were prepared by the same procedure.

Absorption measurements

Absorption measurements were carried out on 37 μm thick samples with a Cary Variant Bio 50 spectrometer. The absorption coefficient α is given by $\alpha = \ln(10)A/d$, where A is the measured absorbance and d the thickness of the film.

Differential Scanning Calorimetry (DSC)

The glass-transition temperature of the materials was determined by a Mettler Toledo calorimeter, model 821^e, calibrated through the melting-point of indium. Materials were measured from −50° to 180°, applying a heating rate of 20 K min^{-1}.

Holographic experiments

The holographic properties of the PPCs were investigated by the common degenerate four-wave-mixing (DFWM) and two-beam-coupling (2BC) technique. All measurements were carried out at 830 nm and a moderate total external light intensity of $I_{ext} = 0.64$ W cm^{-2}. The s-polarized write beams were incident onto the positively biased electrode at an angle of 50° (70°) for write beam 1 (2) relative to the sample normal, which corresponds according to Snell's Law and assuming n(polymer) = 1.7 to an internal angle $\alpha_1 = 26.8°$ ($\alpha_2 = 33.6°$) inside the material. Ultimately, this yields a hologram tilt angle of $\Psi = 30.6°$ and a grating period of $\Lambda = 4.1$ μm. The external intensities were adjusted such that the internal index contrast was $m \approx 1$.

The recorded index grating was probed by a weak p-polarized read beam (approx. 3 mW cm^{-2}), counterpropagating write beam 1. This leads to a transmitted component RB_{trans}, counterpropagating write beam 1, and a diffracted component RB_{diff}, counterpropagating write beam 2, whose intensities were recorded by standard Si-photodiodes (I_t and I_d, respectively) in addition to both transmitted write beam intensities (I_{WB_1} and I_{WB_2}). The internal diffraction efficiency η_{int} is given by:

$$\eta_{int} = \frac{I_d}{I_d + I_t}, \quad (1)$$

the external diffraction efficiency by:

$$\eta_{ext} = \exp\left(-\frac{\alpha d}{\cos \alpha_1}\right)\eta_{int}, \quad (2)$$

with α the absorption coefficient of the composite. The 2BC gain coefficient Γ is defined as:

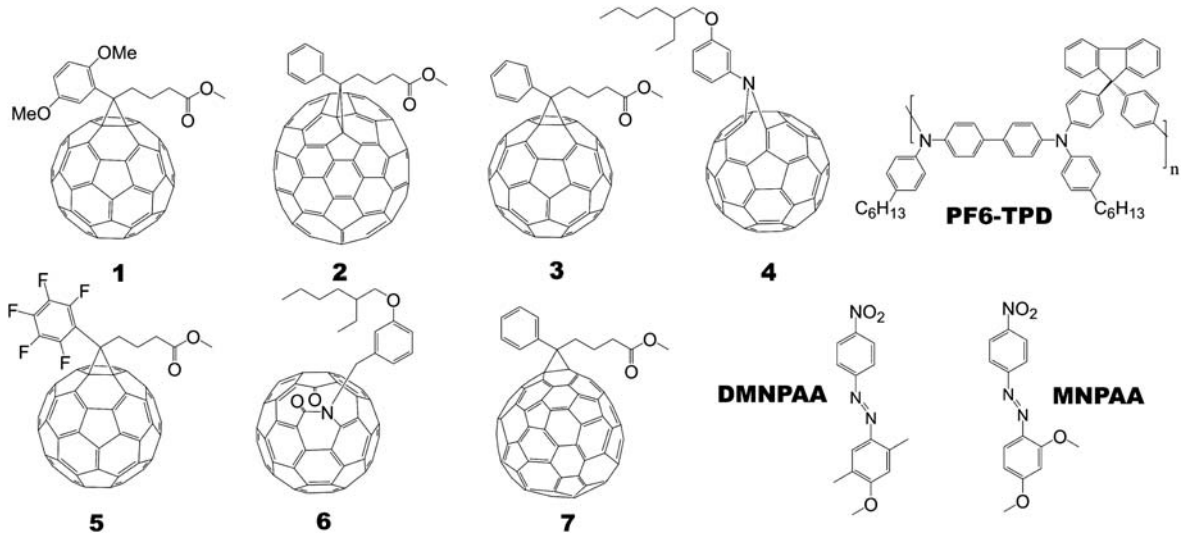

Fig. 1 Chemical structures of fullerene sensitizers, 2,5-OMe-[60]PCBM **1**, [70]PCBM **2**, [60]PCBM **3**, azafulleroid **4**, F5-[60]PCBM **5**, ketolactam **6**, [84]PCBM **7**, hole-conducting polymer PF6-TPD and electro-optic chromophores DMNPAA/MNPAA.

$$\Gamma = \frac{1}{d}\left[\cos\alpha_1 \ln\left(\frac{I_{\mathrm{WB}_1}(E)}{I_{\mathrm{WB}_1}(E=0)}\right) - \cos\alpha_2 \ln\left(\frac{I_{\mathrm{WB}_2}(E)}{I_{\mathrm{WB}_2}(E=0)}\right)\right] \quad (3)$$

Steady-state data were collected at a given electric field E_{ext} and after 60 s of exposure to both write beams. With increasing E_{ext}, the diffraction efficiency first increases, reaches a maximum, and then decreases again (see ESI, Fig. S1†). The field necessary to reach the maximum is referred to as $E(\eta_{\max})$ and is a qualitative measure for the performance of organic photorefractive materials: the lower $E(\eta_{\max})$, the better the PR performance. At $E(\eta_{\max})$ and considering the holographic recording geometry described above, the index modulation amplitude amounts to $\Delta n = 3.4 \times 10^{-3}$.

All dynamic measurements were carried out at $E = 56.6\ \mathrm{V\ \mu m^{-1}}$ applied dc-field. The samples were pre-poled for 60 s and then the write beams were switched on. For pre-illumination experiments, the sample was illuminated uniformly for 1 s applying $0.7\ \mathrm{W\ cm^{-2}}$ of 633 nm non-polarized light 100 ms prior to the actual measurement. The pre-illumination beam was incident perpendicular to the surface onto the negatively biased electrode. For comparison of the dynamic behaviour of the material, we use τ_{50} as a simple qualitative measure of the recording speed, which states the time necessary to reach 50% of the steady-state diffraction efficiency. We refrain from interpreting this number in light of a physical model for the recording process.

Here, the holographic sensitivity S of a material is defined as:

$$S = \frac{\sqrt{\eta_{\mathrm{ext}}(t_{\mathrm{exp}})}}{I_{\mathrm{WB}_{\mathrm{ext}}} t_{\mathrm{exp}}}, \quad (4)$$

where $\eta_{\mathrm{ext}}(t_{\mathrm{exp}})$ is the external diffraction efficiency after a certain exposure time t_{exp}. The time necessary to reach 1% external diffraction efficiency was used to calculate S.

Photo-EMF measurements

Photo-EMF measurements were performed in reflection geometry, *i.e.*, two counter-propagating beams from a He–Ne laser ($\lambda = 633$ nm) with nearly equal intensity illuminate the sample from opposite sides, creating an interference pattern with the period $\Lambda = \lambda/2n \approx 0.19\ \mu\mathrm{m}$. No external field is applied to the sample during this measurement. The average incident intensity I_0 was $0.9\ \mathrm{mW\ cm^{-2}}$. A sinusoidal phase modulation with the amplitude $\Delta = 0.5$ rad was introduced by an electro-optic modulator (Conoptics 350-105). The p-EMF current $J^{\Omega}_{\mathrm{pEMF}}$ signals were detected by a digital lock-in amplifier (Stanford Research SR-830) as a voltage drop at the 100 kΩ load resistance R_{L}. A detailed description of this technique can be found in ref. 22. It was shown in a previous publication[23] that measuring the dependence of $J^{\Omega}_{\mathrm{pEMF}}$ on the external frequency of the applied modulation Ω, allows the determination of two characteristic cut-off frequencies, which are related to the dielectric relaxation time τ_{di} and photo-carrier lifetime τ of the material.

Electrochemistry

Cyclic voltammetry measurements were performed using an Autolab PGStat 100. We used a 1 : 4 mixture of acetonitrile and 1,2-dichlorobenzene as the solvent and tetrabutylammonium hexafluorophosphate (Bu_4NPF_6, 0.1 M) as the supporting electrolyte. The working and counter electrodes were Pt wire, the reference electrode was a Ag wire. The scan rate was $100\ \mathrm{mV\ s^{-1}}$. The potentials were calibrated *versus* ferrocene/ferrocenium (Fc/Fc^+) reference redox couple.

Results and discussion

All PPCs feature complete internal diffraction efficiency (≥88%), and within the accuracy of the experiment similar $E(\eta_{\max})$ are obtained in all cases ($61 \pm 3\ \mathrm{V\ \mu m^{-1}}$, see Table 1). This indicates a similar refractive index modulation Δn and space-charge field E_{SC} for all investigated materials. Moreover, the steady-state gain coefficients Γ within the series are constant within experimental errors ($32 \pm 4\ \mathrm{cm^{-1}}$, Table 1). Together, these findings hint towards a constant phase-shift for all materials, which is equivalent to a constant hole-displacement distance and,

Table 1 Physical data for the investigated sensitizers and PPCs based on them: first reduction potential $E_{1/2,red}$ *vs.* ferrocene/ferrocenium, molar mass M, density of sensitizing molecules in the composite relative to the reference composite $N_S/N_S^{[60]PCBM}$, absorption coefficient α_{830}, field necessary to reach over-modulation of diffraction efficiency $E(\eta_{max})$, and 2BC gain measured in steady-state at 56.6 V μm^{-1}

	M/g mol^{-1}	$N_S/N_S^{[60]PCBM}$	$E_{1/2,red}$/V	α_{830}/cm^{-1}	$E(\eta_{max})$/V μm^{-1}	Γ_s/cm^{-1}
1	970	0.94	−1.106	6	63	28
2	1030	0.88	−1.089	5	61	29
3	910	≡1.00	−1.084	8	63	29
4	953	0.95	−1.058	12	64	27
5	1000	0.91	−1.042	6	58	36
6	985	0.92	−0.918	16	61	30
7	1199	0.76	−0.730	68	58	29

according to the photorefractive theory,[6] a similar trap density under steady-state conditions in all investigated materials. It is interesting to note that the consistency of the data trend is also valid for the [84]PCBM sensitized material, even though it features a significantly higher absorption compared with the other sensitizers (Table 1). This might be due to the fact that the influence of the higher absorption is compensated by the lower number density of [84]PCBM molecules in 1 wt% concentration, which amounts to only 76% of [60]PCBM in the reference composite because of its higher molecular weight.

Despite the essentially identical steady-state performance of the materials, we found a strong influence of the sensitizer on the holographic recording dynamics. Fig. 2a (closed symbols) shows the holographic response time τ_{50} as a function of the reduction potential of the fullerene sensitizer (Table 1). Clearly, the recording speed is the faster the lower the reduction potential, *i.e.*, the higher the acceptor strength of the fullerene. Overall, τ_{50} is reduced by more than one order of magnitude from the weakest to the strongest electron acceptor, the difference in reduction potential being *ca.* 400 mV. In order to assign the increase of the materials' dynamic performance to a discrete physical property, it is necessary to identify the speed limiting process, *e.g.* the photoconductivity of the sample or the rotational mobility of the chromophores.

The fastest response time is roughly 50 ms (sample sensitized with [84]PCBM). By contrast, the chromophore re-orientation time as determined by transient ellipsometry[6] is faster (<20 ms) and essentially the same in all PPCs. This is expected considering the fact that T_g of all materials studied here is identical (6 ± 1 °C), which is indicative of a comparable free internal volume. Intensity-dependent measurements on the [60]PCBM and [84]PCBM sensitized materials (not shown) reveal a sublinear dependence of the holographic recording speed on the irradiance, which in addition to the ellipsometry data excludes orientational mobility limitations on the performance of the materials. Thus, the holographic recording is limited by the photoconductivity of the materials alone. Please note that the photoconductivity of the composites is a convolution of the charge generation, transport, trapping and recombination (see Fig. 3).

In addition to the dynamic measurements described above, all materials were subjected to pre-illumination studies[3,14,24] using short-wavelength light (633 nm) prior to the NIR hologram writing process. In a TPD-PPV-based composite pre-illumination was found to reduce τ_{50} by a factor of 40.[3] This enhancement

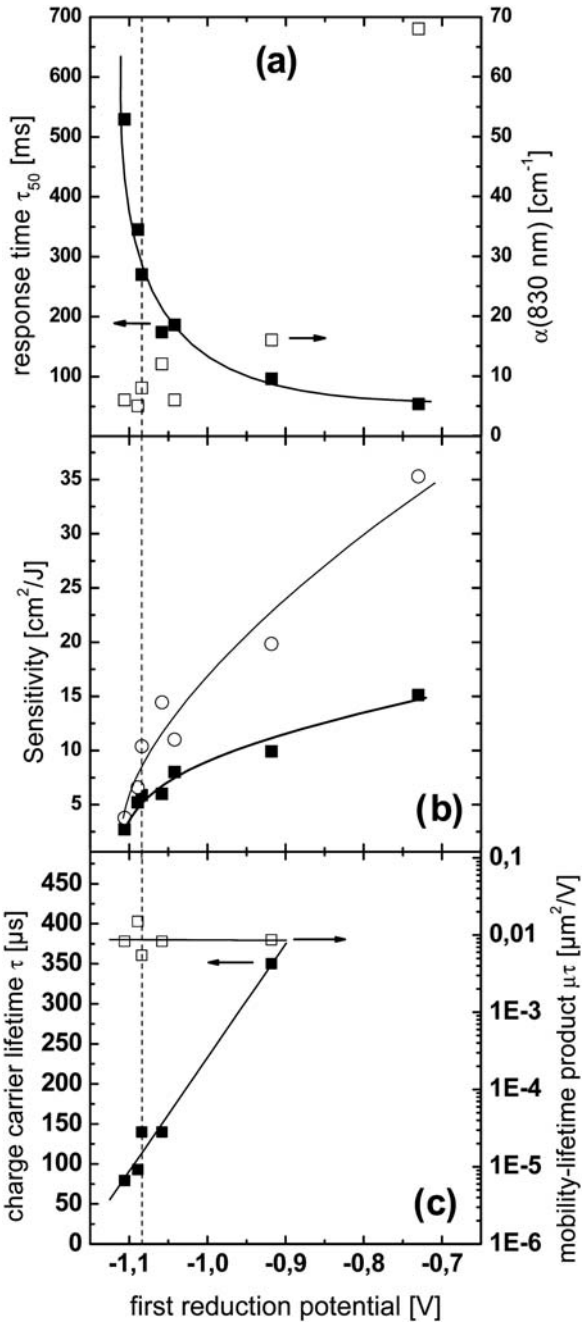

Fig. 2 Physical properties of the PPCs as a function of the reduction potential of the fullerene sensitizer. (a) Holographic response time τ_{50} at $E_{ext} = 56.6$ V μm^{-1} (closed symbols) and absorption coefficient α (830 nm) (open symbols). (b) Holographic sensitivity $S_{1\%}$ calculated according to eqn (4) for 1% external diffraction efficiency, plotted for non-preilluminated (closed squares) and pre-illuminated materials (open circles). (c) Charge carrier lifetime τ (closed symbols) and mobility lifetime product $\mu\tau$ (open symbols) as determined by p-EMF at 633 nm. All lines are guide to the eye. The vertical dashed line indicates the [60]PCBM reference.

was attributed to the spatially homogeneous density of charges, consisting of trapped holes and ionized sensitizer radical anions, present in the material prior to the actual holographic recording process.[25]

For the materials studied here, pre-illumination was found to affect the hologram build-up in all cases, giving rise to a faster

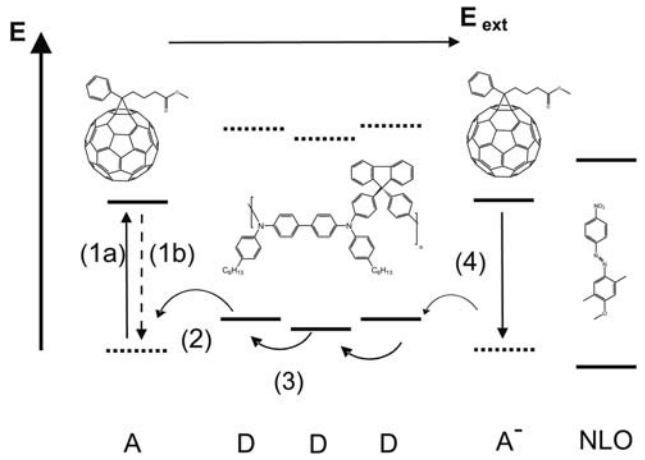

Fig. 3 Energy diagram for the processes involved in the formation of a space-charge field in our PPC. Relative electronic levels of the donor PF6-TPD (D), the fullerene sensitizer (A) and the NLO chromophore DMNPAA (NLO). Arrows indicate the direction of electron movement. Mechanism according to ref. 26: (1a) absorption of the fullerene sensitizer and exciton formation, (1b) geminate recombination, (2) field dependent charge separation, (3) hopping of the hole along the polymer-chain and (4) recombination of hole with fullerene radical anion (A^-).

onset of diffraction efficiency, but reaching steady-state diffraction efficiency and thus saturation of E_{SC}, on a longer timescale compared to non-preilluminated measurements (see ESI, Fig. S1b†). The effect was found to be reversible.

In Fig. 2b, the sensitivity of the PPCs is plotted against the reduction potential of the incorporated fullerene sensitizer upon pre-illumination (open symbols) and of non-preilluminated (closed symbols) materials. The impact of pre-illumination is clearly gaining importance for stronger electron acceptors (the ratio of the sensitivity with and without pre-illumination is depicted in the ESI†), which indicates that a higher charge carrier density is present in the materials before space-charge field formation.

At this point we can clearly exclude any transport limitations on the dynamic performance of the materials. If the photoconductivity would be limited by the transport of holes (step 3, Fig. 3), no performance increase would be expected by pre-illumination. Thus, the dynamics in our PPCs could be either limited by the generation of charge carriers (steps 1a and 2, Fig. 3) or by the recombination of holes with sensitizer radical anions (step 4, Fig. 3), both of which eventually determine the yield of separated charges upon pre-illumination at the beginning of the temporal measurement. Please note that it is not possible to attribute the actual physical mechanism by holographic measurements alone.

In order to clarify the impact of the sensitizers' reduction potential on the photoconductive properties of the materials, all blends except the PPCs sensitized by F5-PCBM and [84]PCBM, the latter being too strongly absorbing at 633 nm, were characterized by the p-EMF technique.

The average photoconductivity, which is proportional to the product of the lifetime τ of the mobile charge-carrier (in this case holes), their mobility μ, and the charge generation rate g, is found to be constant within the series of materials. At the same time, the mobility-lifetime product ($\mu\tau$-product) remains essentially constant (see Fig. 2c). On the one hand, the latter result was expected due to the constant performance of the investigated materials under steady-state holographic conditions (see above). On the other hand, this also renders the charge generation rate g constant within the sensitizer series. Consequently, this finding clearly excludes the charge generation step as the origin of the enhancement of the temporal characteristics of the PPCs in this study.

Fig. 2c shows a linear increase of the charge-carrier lifetime with decreasing reduction potential of the electron acceptor. Obviously, the increased electron affinity of the incorporated sensitizer leads to a lowering of the recombination rates of the photogenerated charge carriers, which is equivalent to an increased charge-carrier density under constant illumination conditions. Thus, the space-charge field corresponding to a certain diffraction efficiency ($\eta_{int} = 50\%$ or $\eta_{ext} = 1\%$) is reached on a shorter timescale, which results in the acceleration of the holographic dynamic response in DFWM-measurements. The p-EMF results indicate that the material performance in this study is limited by charge-carrier recombination. As suggested above, the same may then hold true for the influence of pre-illumination.

The comparison of the constant $\mu\tau$-product and the increased charge-carrier lifetime τ implies that the hole (hopping) mobility (step 3, Fig. 3) decreases as the reduction potential of the sensitizer decreases. The reduction of the recombination rate γ_R with reduced mobility is expected from the description of the Langevin recombination process,[25] which in the case of monopolar charge transport takes the form $\gamma_R = \mu e/\varepsilon\varepsilon_0$, with e the elementary charge, ε the relative static permittivity and ε_0 the permittivity of vacuum. Within the range of investigated sensitizers, this drop in hole-mobility obviously did not influence the performance of the holographic materials through imposing transport limitations on the space-charge field formation (*e.g.* still faster than the rate-limiting step).

It should be pointed out that earlier investigations of the impact of different sensitizers on the photoconductive and photorefractive properties of PPCs[7,8] did not find a distinct influence of the reduction potential on the temporal holographic behavior of the composites. Instead, changes in the dynamic performance of these composites were found to be dominated by changes in the charge generation step. This is presumably due to the rather broad selection of different sensitizer molecules, regarding chemical structure (quinones, tetracyanobenzene and trinitrofluorene)[7] and molecular weight (factor > 3 within the series of ref. 8). In both cases, the utilization of 633 nm as holographic recording wavelength leads to a predominantly absorption related change in temporal response. This may have concealed any influence of the electron affinity and thus the recombination dynamics of the sensitizer radical anion species on the temporal behavior of the composites.

In contrast, except for [84]PCBM, the variations of absorption coefficients and molecule densities of the sensitizers investigated in this study are rather small (see Table 1). Moreover, it is well-known that in low-dielectric amorphous solids, the charge generation (steps 1a followed by 2, Fig. 3) is critically influenced by the separation distance between donor and acceptor moieties.[20] Since at least all C_{60}-based sensitizers have similar size (even considering the solubilizing side groups) and due to the spherical shape of fullerenes in general, we believe that this influence can be neglected here, but may be of significant importance in the results of previous investigations.

Conclusions

In conclusion, we have reported on PPCs based on the hole-conducting polymer PF6-TPD with highly favorable NIR sensitivity due to efficient sensitization by a series of fullerene derivatives. We demonstrate that the holographic recording speed improves by one order of magnitude when lowering the reduction potential of the sensitizer by 400 mV, while all other physical parameters of the materials are essentially identical. This speed increase is attributed to a decrease in the recombination rate, as verified by photo-EMF measurements. Further, the lifetime of the mobile charge carriers (holes) correlates linearly with the reduction potential, while the $\mu\tau$-product and the average photoconductivity g remain essentially unchanged. Pre-illumination was found to have a beneficial impact on the sensitivity of the materials, in particular for the materials using a strong acceptor as sensitizer. All together, the PPCs reported here feature the currently highest photorefractive sensitivity at 830 nm, which makes them very attractive for biomedical applications such as HOCI. The PF6-TPD based materials even outperform the previously most sensitive material based on TPD-PPV[3] (sensitivity of 4 (18) $cm^2\ J^{-1}$ without (with) pre-illumination) under exactly the same measurement conditions.

Acknowledgements

The authors acknowledge experimental support by Jacek Prauzner and fruitful discussions with Dr Malte C. Gather and Dr Jürgen Schelter (all University of Cologne). This work was supported by the European Space Agency (ESA, MAP AO 99-121) and the Germany Ministry of Science and Education (BMBF, project 50WB0730).

Notes and references

1 S. Tay, P. A. Blanche, R. Voorakaranam, A. V. Tunc, W. Lin, S. Rokutanda, T. Gu, D. Flores, P. Wang, G. Li, P. St Hilaire, J. Thomas, R. A. Norwood, M. Yamamoto and N. Peyghambarian, *Nature*, 2008, **451**, 694–698.
2 D. Ishikawa, A. Okamoto, S. Honma, T. Ito, K. Shimayabu and K. Sat, *Opt. Rev.*, 2007, **14**, 246–251.
3 E. Mecher, F. Gallego-Gomez, H. Tillmann, H. H. Hörhold, J. C. Hummelen and K. Meerholz, *Nature*, 2002, **418**, 959–964.
4 M. Salvador, J. Prauzner, S. Köber, K. Meerholz, K. Jeong and D. D. Nolte, *Appl. Phys. Lett.*, 2008, **93**, 231114.
5 M. Salvador, J. Prauzner, S. Köber, K. Meerholz, J. J. Turek, K. Jeong and D. D. Nolte, *Opt. Express*, 2009, **17**, 11834–11849.
6 R. Bittner and K. Meerholz, in *Photorefractive Materials and their Applications II: Materials, Springer Series in Optical Science*, ed. P. Günter and J.-P. Huignard, Springer, Berlin, 2006, vol. 114, ch. 13, pp. 419–486.
7 N. Tsutsumi, Y. Ito and W. Sakai, *Chem. Phys.*, 2008, **344**, 189–194.
8 J. W. Oh, I. K. Moon and N. Kim, *J. Photochem. Photobiol., A*, 2009, **201**, 222–227.
9 O. Ostroverkhova, W. E. Moerner, M. He and R. J. Twieg, *Appl. Phys. Lett.*, 2003, **82**, 3602–3604.
10 O. Ostroverkhova, D. Wright, U. Gubler, W. E. Moerner, M. He, A. Sastre-Santos and R. J. Twieg, *Adv. Funct. Mater.*, 2002, **12**, 621–629.
11 S. J. Zilker and U. Hofmann, *Appl. Opt.*, 2000, **39**, 2287–2290.
12 O. Ostroverkhova and W. E. Moerner, *Chem. Rev.*, 2004, **104**, 3267–3314.
13 J. Thomas, C. Fuentes-Hernandez, M. Yamamoto, K. Cammack, K. Matsumoto, G. A. Walker, S. Barlow, B. Kippelen, G. Meredith, S. R. Marder and N. Peyghambarian, *Adv. Mater.*, 2004, **16**, 2032–2036.
14 E. Mecher, F. Gallego-Gomez, K. Meerholz, H. Tillmann, H. H. Hörhold and J. C. Hummelen, *ChemPhysChem*, 2004, **5**, 277–284.
15 E. H. Mecher, C. Bräuchle, H. H. Hörhold, J. C. Hummelen and K. Meerholz, *Phys. Chem. Chem. Phys.*, 1999, **1**, 1749–1756.
16 Y. Wang and A. Suna, *J. Phys. Chem. B*, 1997, **101**, 5627.
17 E. Hendrickx, B. Kippelen, S. Thayumanavan, S. R. Marder, A. Persoons and N. Peyghambarian, *J. Chem. Phys.*, 2000, **112**, 9557–9561.
18 J. Schelter; G. F. Mielke, A. Köhnen; J. Wies; S. Köber, O. Nuyken, K. Meerholz. *Macromol. Rapid Commun.*, DOI: 10.1002/marc.201000125.
19 F. B. Kooistra, J. Knol, F. Kastenberg, L. M. Popescu, W. J. H. Verhees, J. M. Kroon and J. C. Hummelen, *Org. Lett.*, 2007, **9**, 551–554.
20 C. J. Brabec, A. Cravino, D. Meissner, N. S. Sariciftci, T. Fromherz, M. T. Rispens, L. Sanchez and J. C. Hummelen, *Adv. Funct. Mater.*, 2001, **11**, 374–380.
21 F. B. Kooistra, V. D. Mihailetchi, L. M. Popescu, D. Kronholm, P. W. M. Blom and J. C. Hummelen, *Chem. Mater.*, 2006, **18**, 3068–3073.
22 S. Stepanov, in *Handbook of Advanced Electronic and Photonic Materials and Devices*, Semiconductor Devices, ed. H. S. Nalwa, Academic, London, 2001, vol. 2, pp. 205–272.
23 M. C. Gather, S. Mansurova and K. Meerholz, *Phys. Rev. B: Condens. Matter*, 2007, **75**, 165203.
24 M. Salvador, F. Gallego-Gomez, S. Köber and K. Meerholz, *Appl. Phys. Lett.*, 2007, **90**, 154102.
25 L. Kulikovsky, D. Neher, E. Mecher, K. Meerholz, H. H. Horhold and O. Ostroverkhova, *Phys. Rev. B: Condens. Matter*, 2004, **69**, 125216.
26 C. A. Walsh and D. M. Burland, *Chem. Phys. Lett.*, 1992, **195**, 309–315.